

# Does Head Pose Correction Improve Biometric Facial Recognition?

Justin Norman and Hany Farid  
University of California, Berkeley  
Berkeley CA, USA

justin.norman@berkeley.edu and hfarid@berkeley.edu

## Abstract

*Biometric facial recognition models often demonstrate significant decreases in accuracy when processing real-world images, often characterized by poor quality, non-frontal subject poses, and subject occlusions. We investigate whether targeted, AI-driven, head-pose correction and image restoration can improve recognition accuracy. Using a model-agnostic, large-scale, forensic-evaluation pipeline, we assess the impact of three restoration approaches: 3D reconstruction (NextFace), 2D frontalization (CFR-GAN), and feature enhancement (CodeFormer). We find that naive application of these techniques substantially degrades facial recognition accuracy. However, we also find that selective application of CFR-GAN combined with CodeFormer yields meaningful improvements.*

## 1. Introduction

Fueled by the (often un-verified) promise of accurate and automated identity verification, biometric facial recognition systems have become increasingly prevalent in both high stakes commercial and forensic settings [2, 17, 20, 21]. In controlled environments, modern face recognition models often report accuracies exceeding 95%, which has led to public and institutional confidence in their deployment [15, 19, 21]. However, recent research has cast serious doubt on the generalizability of these results to real-world conditions [1, 12, 14, 18], especially in forensic contexts. These systems, while powerful, are not as infallible as often presumed, especially when tasked with matching images of faces captured under non-ideal conditions (e.g., occluded, low-quality, low-resolution, etc.).

A growing body of evidence suggests that images, often characterized by poor resolution, compression artifacts, occlusions, non-frontal and extreme poses, and inconsistent lighting, result in significant challenges to even state-of-the-art recognition systems. Under these conditions, recognition accuracy can drop precipitously, sometimes by more than 30 percentage points compared to performance on

high-quality benchmark datasets [13]. These degradation factors, common in surveillance footage, amateur photography and law enforcement imagery, are not edge cases but rather emblematic of the forensic context.

Given this broader understanding of how and when facial recognition systems fail, a natural question emerges: Can targeted interventions yield meaningful improvements without overhauling the entire recognition pipeline? Rather than attempting to universally enhance all input data, (a strategy shown to introduce artifacts and even reduce accuracy in even ideal conditions) [3, 9, 17, 24], or retrain the underlying recognition models, we explore whether selective, context-aware data preprocessing can offer a practical compromise.

We previously developed a many-to-many, model-agnostic, facial identification system evaluation framework for real-world images in high-stakes use cases [13]. In subsequent work [13], we leveraged this framework to discover the impact of image deblurring and super resolution models on facial recognition systems. We found that naive application of these techniques failed to improve biometric face recognition. In this work, we apply more targeted enhancement and restoration interventions to diverse human face images that have otherwise proven difficult for existing state-of-the-art facial recognition systems.

One such treatment performs a high-fidelity 3D facial mesh reconstruction from a single image via the integration of a CNN encoder and ray tracing [4, 5]. Separately, we attempt a second full facial reconstruction process, which performs face frontalization and de-occlusion in a single model architecture, utilizing the CFR-GAN optimizer family and library [7]. In order to further increase the fidelity of human features within reconstructed and rectified images, we leverage the CodeFormer human subject restoration model [26]. We also introduce a new classifier to identify specific images that will benefit from these restoration and enhancement techniques.

Overall, we find that some targeted interventions are beneficial in specific circumstances. However these benefits are constrained by several factors, such as the ability to reliably

detect forensic identification failures, overall image quality, subject orientation and restoration technique used. As such, these interventions may only be applicable to specific use cases, have non-trivial requirements, and should not be considered a panacea.

## 2. Forensic Facial Lineups

In previous work [13] we sought to assess the reliability of facial recognition technologies often used in real-world, high-stakes forensic scenarios, particularly when image quality is poor and/or faces are obscured. To do this, we developed a new, model-agnostic forensic evaluation framework for facial recognition systems. We then systematically tested the performance of widely-used facial recognition models, ArcFace and FaceNet using this process. The framework consists of the use of controlled image lineups to examine the impact of lineup composition and confounding factors like facial occlusions and variations in image quality.

These lineups are created by first extracting a vector embedding for each image in the dataset. The five most similar images to the source image – based on embedding distance – are added to the lineup. From there, a random probe image from the same identity as the source is added to the lineup. Using the vector embeddings extracted for each lineup image, the most similar image to the source is computed. If the most similar lineup image to the source is the probe image, then the evaluation for that lineup is considered to be successful; if not then it represents a failure of the facial recognition system.

The study also included a cross-comparison of multiple lineup configurations in order to explore the impact of false positives and negatives under various conditions. Specifically, we constructed controlled facial forensic lineups to systematically evaluate recognition model performance across different scenarios. These lineup configurations varied in terms of image quality (low-resolution vs. high-resolution), occlusion levels (partially-occluded vs. unoccluded faces), and dataset composition. This approach ensured that the evaluation methodology covered multiple lineup structures, ranging from ideal laboratory conditions to challenging real-world forensic scenarios.

To support this work, we leveraged both a real-world dataset, curated from the CASIA-WebFace dataset, and a synthetic dataset created using human-face image-synthesis software. The synthetic dataset in particular, enabled precise control over the conditions under which the images were captured, including varying levels of image degradation, occlusion, and lineup complexity. Specifically, the dataset itself consisted of thousands of synthetic images representing different demographic backgrounds, lighting conditions, and facial poses. We demonstrated that, with proper calibration, synthetic faces could be used as a proxy

for real-world face data, both reducing the challenges of collecting new biometric data, and increasing the diversity of the baseline dataset. However, even working with synthetic data has its potential risks including consent circumvention and diversity washing [22]. Overall, the use of synthetic data allowed for a rigorous analysis of the accuracy and reliability of these models in forensic conditions that mimic real-world challenges.

The results of the forensic framework evaluation research highlight that, while state-of-the-art facial recognition models achieve high accuracy when used under ideal circumstances, their performance significantly degrades under likely real-world forensic conditions. This work specifically highlighted substantial drops in accuracy when images were of low quality, occluded, or when non-probe images in lineups have high similarity to the source identity. These findings underscore the importance of evaluating these systems not just in clean, controlled environments but under realistic conditions to better understand their effectiveness and limitations in forensic applications.

This earlier work advocates for setting realistic standards for the deployment of facial recognition technologies in high-stakes contexts, (such as law enforcement and court proceedings), in order to mitigate potential biases, misuse and inaccuracies.

## 3. Dataset

As in [13], we make use of a single, real-world dataset, derived from the CASIA-WebFace dataset [23]. This dataset consists of 491,414 images from 10,575 identities. Each image is of various size, quality, pose, subject clothing, and environment. We were forced to impose some manual curation due to the initial quality of the dataset. This curation included: the removal of duplicate images, incorrectly labeled images and images which do not contain a human face.

This dataset is significantly larger than the original dataset utilized in our previous research [13, 14], which consisted of approximately 37,500 images from 7,500 identities.

### 3.1. Creating Lineups

The increased scale of the dataset required some key changes to our evaluation framework, as our original implementation was not designed to efficiently handle such a large dataset. On a single-GPU workstation, brute force processing the expanded dataset through the evaluation framework would take at least 21 hours per run. Under this configuration, running the entire accuracy pipeline – including embedding extraction, similarity computation, lineup generation and accuracy scoring – was computationally prohibitive.

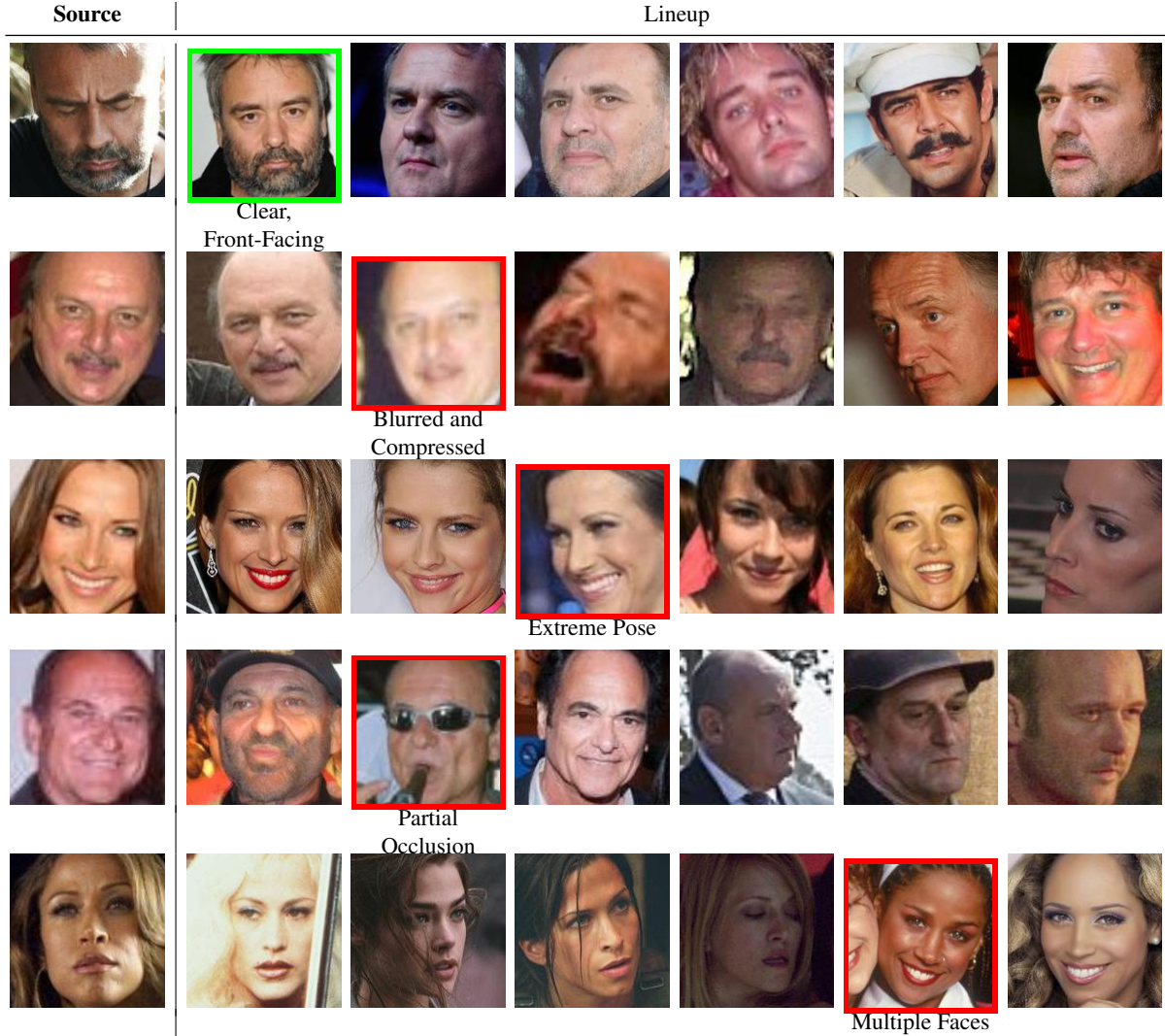


Figure 1. Facial recognition lineup examples showing one successful match (top row) and four failures. Each row displays a source image (left) followed by the constructed lineup. Green borders indicate successful recognition where the probe with the same identity as the source is correctly ranked first; red borders on the probe image indicate that the probe image was not correctly matched.

Our most substantial technical enhancement was the replacement of this brute-force similarity computation-based lineup generation process with Facebook AI Similarity Search (FAISS) for efficient embedding similarity computation [6]. Our original pairwise similarity approach scaled quadratically with dataset size, becoming computationally prohibitive as data volumes increased. FAISS addresses this through optimized indexing for high-dimensional vectors, enabling sub-linear similarity search through its IndexFlatIP structure. We also implement L2-normalization on all embeddings and process queries in batches of 256, allowing FAISS to compute similarities efficiently through vectorized operations. This optimization reduced overall processing time from 21 hours to approximately one hour

per run, while maintaining comparable accuracy.

We also implemented an intelligent caching system that stores and loads embeddings strategically as needed. This is complemented by active memory management that ensures efficient resource utilization when working with GPU resources for embedding generation and similarity computations. After similarity computation, we then perform final lineup assignment for each sample, leveraging the FAISS and caching efficiencies. These improvements enabled us to accurately generate lineups for the full dataset processing, while maintaining reasonable computational requirements and execution times.

In the original evaluation framework, both recognition systems demonstrated strong performance: ArcFace



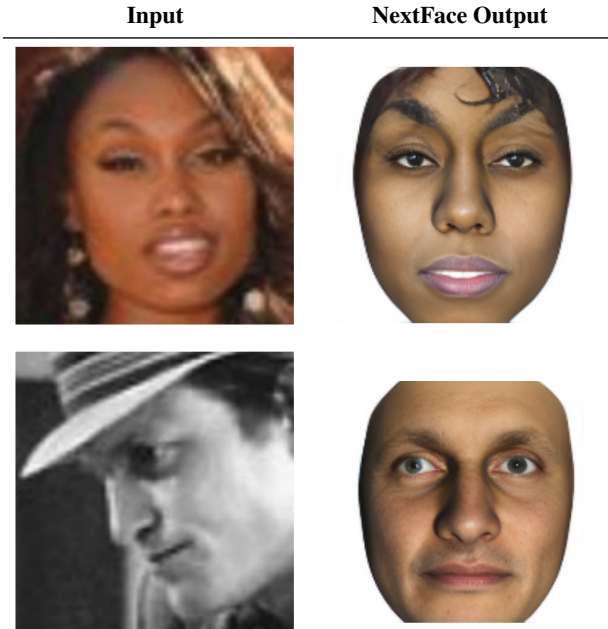


Figure 2. NextFace frontalization.



Figure 3. CFR-GAN frontalization.

achieved 82.3% accuracy and FaceNet achieved 72.3% accuracy. These results established a baseline understanding of recognition system capabilities under the initial test conditions. When evaluated using our expanded framework, with a more diverse and comprehensive dataset, both systems showed modest improvements in accuracy. ArcFace’s accuracy increased to 89.7%, representing a gain of 7.4 percentage points. FaceNet’s accuracy rose to 76.9%, an improvement of 4.6 percentage points.

Critically, despite the substantially larger and more diverse dataset in the expanded framework, the overall accuracy levels remained fairly similar to the original evaluation. This consistency suggests that both models maintain robust performance across varying dataset sizes and compositions.

This new evaluation framework, combined with a larger dataset, allows us to begin efficiently exploring state-of-the-art methods for head-pose correction.

## 4. Head-Pose Correction

The ability to reconstruct a high-quality image from a severely degraded or damaged image has emerged as a growing and crucial area of study within the field of computer vision. Contributions such as Krishnan et al.’s exploration of blind deconvolution to recover sharp images from blurred ones [10] and Zamir et al.’s Restormer model [25], are examples of technological and algorithmic improvements which have driven a major shift in image restoration.

As shown in our previous work, image enhancement models, (even those tuned specifically for human body/face

reproduction), can introduce both perceptually visible and invisible artifacts, which are then harmful to future recognition tasks [14].

One of the main attributes that can make an image challenging for face recognition models is the subject’s pose within the image. Frontal-facing images make up the majority of most models’ training data and, as such, are more likely to be successful in facial identification and recognition tasks. However, most real-world data and datasets contain a high variance of head and body poses, which often prove challenging for facial recognition models.

In addition to pose, partial occlusion of faces is another challenge for facial recognition and identification models. Occlusion can occur as a result of subject position, scarves, hats, or sun-glasses. Any of these occlusions will result in less information available for face feature extraction during a recognition task.

### 4.1. 3D Head Pose Correction (NextFace)

In 2021, Dib et al. introduced a self-supervised learning approach for monocular face reconstruction that captures high-fidelity geometry, reflectance, and illumination from complex scenes [5]. Their method integrates a CNN encoder with a differentiable ray tracer, which effectively captures intricate lighting effects and facial features, such as diffuse and specular albedos and self-shadows. This ray tracing-based approach is more robust than previous methods and as shown in Figure 2 yields a realistic morphable face model from a single image.

This model stands out among other contemporary techniques by handling computational ray tracing during training, resulting in an efficient inference phase that preserves detailed facial attributes while maintaining near real-time performance. It avoids landmark dependencies typically used in optimization-based methods, improving robustness and adaptability for varied conditions. This high-quality reconstruction also facilitates practical applications, including facial relighting and removal of self-shadows, illustrating its broad applicability in computer vision tasks.

#### 4.2. 2D Head Pose Correction (CFR-GAN)

Recently, generative computer-vision models, such as the Complete Face Recovery GAN [7] seek to “rectify” extreme pose face images to a neutral profile pose by effectively combining 2D face reconstruction, texture swapping, self-supervised learning, and generative adversarial training to simultaneously solve the challenging problem of joint face rotation and de-occlusion. As illustrated in Figure 3, this process results in high-quality, occlusion-free images that can be used for various downstream face-related tasks.

#### 4.3. Lineup Accuracy after Head-Pose Correction

Surprisingly, the 2D and 3D restoration approach led to a significant degradation in overall facial recognition accuracy. When lineup images were restored using CFR-GAN accuracy for FaceNet was 58.7% and 80.4% for ArcFace. By comparison, baseline performance of for FaceNet and ArcFace was 76.9% and 89.7%. When lineup images were restored using NextFace, accuracy declined even further to 25% for FaceNet and 43.4% for ArcFace. Overall these results suggest that these head-pose correction techniques, while improving visual quality, appear to remove or distort distinctive facial features necessary for accurate facial recognition.

These results motivate closer examination of the restored images themselves. Visual inspection of the CFR-GAN and NextFace outputs, Figures 2 and 3, reveal substantial artifacts and distortions, particularly in cases where the input images deviated significantly from frontal orientation or contained occlusions. CFR-GAN frequently introduced blurring artifacts that homogenize distinctive facial textures. NextFace, despite its sophisticated geometric normalization capabilities, occasionally produced warped facial structures when confronted with extreme pose variations. In addition, NextFace does not include the neck or shoulder profile of any subject, Figure 2. These observations led us to investigate a potential solution.

#### 4.4. 2D Restoration (CodeFormer)

Since both NextFace and CFR-GAN resulted in the introduction of significant subject artifacts, we explored the introduction of a secondary image restoration tech-

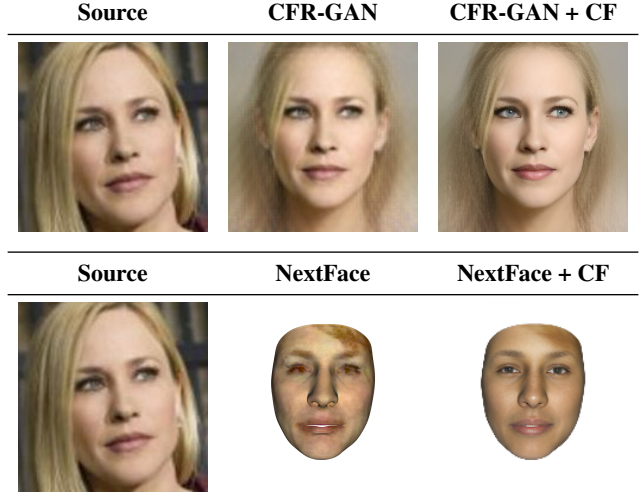


Figure 4. CFR-GAN frontalization followed by CodeFormer (CF) enhancement (top row) and NextFace frontalization followed by CF (bottom row).

nique. Approaches such as the CodeFormer codebook-lookup transformer model [26] seek to increase the fidelity of low quality images by passing a degraded image through a feature extraction module. These features are then processed by CodeFormer, a Transformer-based prediction network, which leverages a learned discrete codebook to represent high-quality facial attributes. The codebook serves as a compact, discrete space for face representation, where CodeFormer predicts the sequence of code entries that best reconstruct the high-quality version of the face. The discrete codebook lookup helps reduce the ambiguity often found in mapping degraded inputs to restored outputs, providing a set of optimal visual atoms for restoration. Furthermore, a controllable feature transformation module is used to balance fidelity and quality, allowing the user to control the level of enhancement applied to the facial image. In our implementation, CodeFormer was configured with a codebook size of 1,024 entries, embedding dimension of 512, an 8-head transformer with 9 layers, and skip connections at resolutions [32, 64, 128, 256]. The controllable feature transformation weight  $w$  was set to 0.7, balancing fidelity to the original degraded image against enhancement quality. Face detection utilized RetinaFace with a ResNet-50 backbone, aligning faces to  $512 \times 512$  pixels with an eye distance threshold of 5 pixels. Background regions were upsampled  $2 \times$  using RealESRGAN (tile size 400, padding 40), and the final restored output was resized to  $160 \times 160$  pixels to match the original cropped face dimensions in our dataset. The result is a restored, high-quality face image, which maintains natural facial attributes while improving visual quality. Shown in Figure 4 are examples of applying CodeFormer after head-pose estimation.

#### 4.5. Lineup Accuracy after Head-Pose Correction and Restoration

In order to determine the effectiveness of restoration techniques in improving recognition model performance on the evaluation framework, we created three new variants of our evaluation dataset. Each variant contained lineup images, (excluding source images), which were processed through a different restoration approach: CFR-GAN alone, NextFace alone, CFR-GAN combined with CodeFormer and NextFace combined with CodeFormer. We then applied the evaluation pipeline to these restored datasets.

Running the evaluation on NextFace and CodeFormer yielded an accuracy of 56.6% using ArcFace and 46.4% using FaceNet. This result, while an improvement from the baseline NextFace-only performance of 43.4% for FaceNet and 25% for ArcFace, it is still well below the non-corrected baseline. As a result, we chose to discontinue use of this head-pose restoration technique.

However, the combination of CFR-GAN with the CodeFormer model resulted in accuracy improvements over the non-corrected baselines of 82.3% and 72.3% for ArcFace and FaceNet respectively. This two-stage approach: first applying geometric correction through CFR-GAN, then enhancing facial features through CodeFormer’s learned codebook, proved more effective than either technique alone. Given NextFace’s poor standalone performance and our superior results with the CFR-GAN + CodeFormer pipeline, we focused our subsequent analysis on this combined approach.

Our investigation into the effectiveness of the CFR-GAN + CodeFormer image restoration pipeline yielded promising results across a large-scale evaluation of 30,535 lineups. The restoration process demonstrated a success rate of 31.9%, improving nearly one-third of the processed lineups. Of these, 9,749 lineups showed improvement in probe ranking while 20,786 remained unchanged, Table 1.

To quantify the impact of restoration, we measured the change in probe image ranking within each lineup. In our evaluation framework, each lineup consists of six candidate images ranked by similarity to the source image, with rank 0 (first position) being the most similar. A successful restoration moves the true probe image closer to rank 0, while an unsuccessful restoration may push it further down the ranking Table 1.. For unsuccessful restorations, we observed an average rank change of 0.53 positions, meaning that failed restoration attempts typically moved the probe image approximately half a position worse in the ranking.

The distribution of rank changes followed a roughly normal distribution with a positive skew, where 29.3% of lineups showed positive movement and 21.7% remained unchanged. Notably, positive position changes occurred more frequently than negative ones, suggesting the potential for targeted application of the restoration pipeline. These

Table 1. Distribution of Lineup Rank Changes for CFR-GAN + CodeFormer

Rank Change	Number of Lineups	Percentage
-5 positions	1	0.01%
-4 positions	443	1.45%
-3 positions	932	3.05%
-2 positions	1,530	5.01%
-1 positions	2,315	7.58%
No change	6,629	21.71%
+1 positions	2,816	9.22%
+2 positions	2,153	7.05%
+3 positions	2,072	6.79%
+4 positions	1,895	6.21%

findings demonstrate that the CFR-GAN + CodeFormer pipeline can effectively improve image ranking positions when applied selectively.

The results suggest that implementing a screening process to identify optimal candidates for restoration could significantly enhance the pipeline’s effectiveness. Throughout this stage of the project, we had access to ground truth data for each lineup. This provides the ability to only apply the restoration pipeline directly to failure cases and not success cases. However, in real-world cases, we would not know if an intervention is needed.

## 5. Predicting Failure

Analysis of the results from the correction and restoration process establish that CFR-GAN + CodeFormer can potentially improve accuracy. However, when this treatment is applied to successful lineup identifications, 60% of those same lineup identifications fail. As such, operational deployment requires the ability to predict potential biometric lineup failures ahead of time.

### 5.1. Dataset

We developed a machine-learning approach to predict lineup failure. Our model was trained on a subset of the original CASIA-WebFace dataset, processed through the forensic lineup task, consisting of 244,825 unique lineup images from failed lineup identifications. This smaller dataset was first curated using Dlib [8] and Mediapipe’s Holistic [11] to remove images with unnatural body poses, total obfuscation of faces, as well as extreme brightness, darkness or blur. The resulting dataset had a class imbalance with a 12.5% lineup failure rate, as opposed to the overall dataset failure rate of 33%. The initial training dataset split magnitudes were: 176,274 samples (72%) for training, 19,586 samples (8%) for validation, and 48,965 samples (20%) for final evaluation.

To address the inherent class imbalance, we gener-



ate multiple rebalanced training datasets using controlled undersampling of the majority class. Precision-focused datasets employ conservative ratios ranging from 1.2:1.0 to 2.0:1.0 (success:failure), creating 10 distinct training sets with failure rates between 33% and 45%. Recall-focused datasets use more aggressive ratios from 0.7:1.0 to 1.1:1.0, yielding failure rates between 48% and 59%. Each rebalanced dataset maintains the original minority class samples while randomly sampling the majority class according to the target ratio. Deterministic random seeds ensure reproducible sampling across training runs.

## 5.2. Feature Engineering

The lineup-failure prediction model combines deep-learning embeddings with traditional image quality metrics, capturing both semantic content and low-level visual characteristics.

The deep-learning features consist of a 768-D OpenCLIP embeddings that encode high-level facial semantics and contextual information. These embeddings are extracted using the ViT-B/32 architecture pre-trained on LAION-400M.

Traditional descriptive image features contribute 42 dimensions across six categories. **Lighting** (6 features): grayscale mean, standard deviation, Shannon entropy from 256-bin histogram, dark/bright pixel ratios (thresholds 50, 200), and Laplacian variance. **Quality** (7 features): local contrast via Sobel diagonal gradient, histogram-weighted global contrast, percentile-based dynamic range (5th-95th), Michelson contrast, RMS contrast, and standard deviation. **Noise** (5 features): diagonal pixel difference standard deviation, SNR in decibels, noise-to-signal ratio, and residuals from  $3 \times 3$  median filtering (standard deviation and mean absolute). **Sharpness** (6 features): Sobel gradient magnitude statistics ( $3 \times 3$  kernels), Laplacian variance, high-frequency FFT energy excluding center radius  $\min(h, w)/4$ , and mean log-magnitude spectrum. **Texture** (2 features): local variance from  $3 \times 3$  averaging kernel and Canny edge density (thresholds 50, 150). **Face geometry** (16 features): detection, count, area/centering ratios, eye and mouth aspect ratios, bilateral symmetry across 23 landmark pairs, and head pose angles extracted using dlib’s 68-point landmark detector. All image operations implemented via OpenCV, with scipy.stats for entropy computation.

The seven quality features encompass multiple contrast formulations including local contrast computed as the variance of combined Sobel operator responses, global contrast derived as  $\sqrt{\sum (i - \mu)^2 \cdot H(i)}$  where  $i$  represents intensity values,  $\mu$  is the mean intensity, and  $H$  is the normalized histogram, dynamic range measured as the difference between 95th and 5th percentile intensities, brightness entropy (repeated from histogram analysis), Michelson contrast calculated as  $(I_{max} - I_{min}) / (I_{max} + I_{min})$  where  $I_{max}$  and  $I_{min}$  are the maximum and minimum pixel inten-

sities, RMS contrast computed as  $\sqrt{\text{mean}((I - \mu)^2)}$  where  $I$  represents pixel intensities, and standard deviation as an additional contrast measure.

The above mentioned five Noise features employ multiple detection strategies including noise sigma estimated from diagonal pixel differences  $\sigma = \text{std}(I[: -1, : -1] - I[1 :, 1 :])$ , signal-to-noise ratio computed as  $10 \log_{10}(P_{signal}/P_{noise})$  where signal power is mean squared intensity and noise power is  $\sigma^2$ , noise-to-signal power ratio, standard deviation of  $3 \times 3$  median-filtered residuals, and mean absolute deviation of median filter residuals. Sharpness and blur detection (6 features) combines spatial and frequency domain approaches through Laplacian variance, mean and standard deviation of gradient magnitudes computed from Sobel operators in x and y directions, high-frequency energy measured from FFT magnitude spectrum excluding the central circular region (radius =  $\min(\text{height}, \text{width})/4$ ), mean FFT magnitude in log scale for blur detection, and a redundant sharpness measure equal to Laplacian variance.

The two texture characterization features capture local structural variation through  $3 \times 3$  kernel-based local variance computation and edge density measured as the proportion of pixels detected by Canny edge detection with thresholds of 50 and 150. Facial geometry measurements (16 features) leverage dlib’s frontal face detector and 68-landmark shape predictor to extract binary face detection status, face count, face area ratio relative to total image area, horizontal and vertical face centering offsets, left and right eye aspect ratios computed as  $(A + B)/(2C)$  where A and B are vertical distances and C is horizontal distance between eye landmarks, average eye aspect ratio, difference between left and right eye aspect ratios, mouth aspect ratio calculated similarly from inner lip landmarks, face symmetry score derived from bilateral landmark pair distance comparisons relative to the nose bridge center, pose angles (roll from eye alignment, yaw from nose deviation, pitch from nose-mouth vertical alignment), and face width and height ratios.

All 810 features undergo standardization using StandardScaler [16] to ensure equal contribution across different scales, with NaN and infinite values replaced by bounded defaults (0.0) and clipping extreme values to  $\pm 1e6$  to ensure numerical stability during model training.

## 5.3. Model Architecture and Training

Our model employs a hybrid two-stage ensemble architecture designed to balance precision, (the proportion of predicted failures that were actual failures), and recall, (the proportion of actual failures that were correctly identified) through complementary model specialization. The approach trains separate cohorts of precision-focused and recall-focused classifiers on our previously mentioned strategically rebalanced datasets, then combines their pre-

dictionaries using geometric mean aggregation.

The ensemble comprises 20 base classifiers organized into two specialized cohorts: 10 precision-focused models and 10 recall-focused models. Each cohort employs four algorithm types: Logistic Regression, Gradient Boosting/Extra Trees, Random Forest, and XGBoost, with hyperparameters tuned for their respective objectives.

**Precision-Focused Models** employ conservative configurations to minimize false positives. These models utilize higher regularization with  $C=1.0$  for logistic regression and implement conservative tree splitting criteria including `min_samples_split=20` and `min_samples_leaf=10`. Class weighting remains minimal at a 1:1.2 ratio to avoid aggressive minority class emphasis, while tree depths are constrained to shallow ranges of 3-8 levels to prevent overfitting to noisy patterns.

**Recall-Focused Models** use aggressive parameterizations to capture subtle failure patterns. These configurations employ reduced regularization with  $C=0.1$  for logistic regression and implement aggressive class weighting up to 1:2.5 ratios to enhance minority class sensitivity. Tree structures are more flexible with `max_depth` ranging from 8-10 levels and reduced `min_samples_leaf` requirements of 5 samples, while gradient boosting algorithms utilize lower learning rates of 0.05 compared to the standard 0.1 to enable more nuanced pattern learning.

The dual-objective design balances conservative and aggressive tendencies through geometric mean probability aggregation.

Models are trained using stratified sampling to preserve class distributions across train/validation/test splits (72%/8%/20%). Each base classifier fits on its assigned rebalanced dataset using algorithm-specific hyperparameters, with training terminating at convergence or maximum iteration limits (2000 for logistic regression, 100 estimators for tree-based methods).

The ensemble aggregation employs geometric mean combination of probability predictions:  $P_{ensemble} = \sqrt{P_{precision} \times P_{recall}}$ , where  $P_{precision}$  and  $P_{recall}$  represent the mean probabilities from precision-focused and recall-focused model cohorts, respectively. This approach balances conservative and aggressive tendencies while maintaining calibrated probability estimates.

Classification thresholds are optimized through grid search across the validation set, evaluating 50 threshold values between 0.25 and 0.75 to maximize a composite score prioritizing both precision and recall above 0.5. The final threshold of 0.42 was selected based on validation performance optimization.

During our training process, we evaluated multiple ensemble strategies including cascading approaches, weighted voting, and various aggregation functions. The geometric mean strategy demonstrated superior performance, achiev-

Table 2. CFR-GAN + CodeFormer Restoration for Previously Failed Lineups

Outcome Category	Count	Percentage
Rank Improvements	877	27.6%
Rank Degradations	324	10.2%
Rank Unchanged	1,977	62.2%
Success Conversions (Rank 0)	221	7.0%
Total Analyzed	3,178	

Table 3. CFR-GAN + CodeFormer Restoration for Previously Successful Lineups

Outcome Category	Count	Percentage
Rank Degradations	31	10.7%
Rank Unchanged	260	89.0%
Failed Restoration	1	0.3%
Total Analyzed	292	

ing the best precision-recall balance with validation metrics of 91.6% precision and 51.8% recall.

Cross-validation using the geometric mean ensemble on the validation set confirmed model stability and generalization capability, with coefficient of variation below 0.05 for both precision and recall across five-fold validation. The final model selection prioritized configurations achieving both precision and recall above 0.5, with secondary optimization for F1-score maximization.

## 5.4. Model Performance

After validation, the model achieved 91.6% precision (defined as the proportion of predicted failures that were actual failures) and 51.8% recall (the proportion of actual failures that were correctly identified), yielding an F1-score of 0.66. This conservative approach was deliberately designed to minimize false positive predictions while maintaining sufficient sensitivity to detect genuine lineup failures.

## 6. Restoration Impact Analysis

After applying the model described in the previous section, the lineup associated with any source image predicted to fail was subject to the complete CFR-GAN + CodeFormer restoration. We then compared the movement of the correct identity in lineup ranking before and after restoration.

Shown in Table 2 are the restoration outcomes for correctly identified lineup failure. Among 3,178 true positive predictions, 877 samples (27.6%) showed rank improvements after restoration processing. Most significantly, 221



samples transitioned from lineup failures before restoration (rank > 0) to perfect matches (rank = 0) after restoration.

These results demonstrate meaningful restoration improvements. True positive cases, where the model successfully identified a lineup failure image and it was restored, showed an average rank improvement of 0.39 positions, with original rankings averaging 1.83 improving to 1.44 after restoration. This represents a 21.3% improvement in average ranking position, indicating substantial quality enhancement for correctly identified failure cases.

Next we analyze the false positive predictions, where the model incorrectly identified an image as a failure when it belonged to a successful lineup. As shown in Table 3, among the 292 incorrectly predicted failures, 260 samples (89%) maintained their original ranking after the restoration processing, and only 31 samples (10.7%) led to an incorrect lineup match. In particular, the original rank of 1.00 increased marginally to 1.11 after the restoration. This minimal impact demonstrates that the restoration pipeline’s conservative application causes limited harm when applied to already successful lineups.

The experimental results validate our failure prediction approach across multiple dimensions. The binary classification model successfully identifies restoration failures with high precision, while the restoration pipeline demonstrates measurable improvements for correctly identified cases. The 27.6% improvement rate among true positives, combined with the minimal negative impact of false positives, establishes a favorable risk-reward profile for automated restoration intervention.

The success conversion rate of 7.0% represents particularly valuable outcomes, as these cases transition from failed restorations to perfect matches in the evaluation framework. When combined with the broader improvement rate, the system demonstrates clear utility for enhancing restoration quality in production environments.

The conservative model design proved appropriate for this application domain, where precision is prioritized over recall to minimize unnecessary processing while ensuring high-confidence interventions yield measurable improvements. The 91.6% precision rate provides sufficient reliability for automated deployment, while the 51.8% recall rate captures a substantial portion of improvable failure cases.

## 7. Discussion

Our results provide a nuanced answer to the question posed in the abstract: *Can targeted, AI-driven head-pose correction and image restoration meaningfully improve facial recognition accuracy in forensic-style conditions?* At a high level, we find that the answer is both yes and no. Naively applied, modern restoration and frontalization tools systematically harm performance, sometimes catastrophically. However, when these same tools are combined

carefully and deployed selectively, they can yield measurable and practically meaningful improvements. This duality highlights the need for a shift in how enhancement technologies are evaluated and operationalized in biometric pipelines, particularly in high-stakes forensic settings.

Our first set of experiments demonstrates that both 3D (NextFace) and 2D (CFR-GAN) head-pose correction, when applied uniformly to lineup images, substantially degrade recognition accuracy relative to an already-strong baseline. This is not simply a small trade-off between visual quality and model robustness; in some conditions, the performance drop is dramatic. NextFace, in particular, reduces accuracy to near-chance levels in our lineup setting, despite producing visually plausible, frontalized faces. These findings reinforce and extend prior work showing that more visually pleasing images do not necessarily translate into better machine recognition performance [14].

These findings caution strongly against the practice of running automatic enhancement on all faces entering a forensic pipeline. Even sophisticated methods with impressive qualitative demos can be actively harmful when composed naively with downstream recognition systems.

In contrast to the failures of naive application, our combined CFR-GAN + CodeFormer pipeline reveals that targeted, two-stage restoration can deliver net gains in recognition accuracy when applied under the right conditions. From a modeling perspective, this combination is appealing: CFR-GAN focuses primarily on geometric normalization (pose correction and de-occlusion), while CodeFormer operates in a learned codebook space to reconstruct high-quality facial detail. This combined approach improves average probe rankings and yields an overall boost in lineup accuracy relative to the non-restored baseline.

Our findings have several implications for the forensic use of facial recognition systems: (1) Agencies and vendors should be wary of marketing or deploying plug-and-play enhancement modules that are applied blindly to all images. Even when they produce visually attractive results, these tools can systematically degrade biometric performance; (2) Restoration methods must be evaluated in the context of the specific recognition systems and tasks with which they will be paired. Improvements in human-perceived image quality or benchmark restoration metrics do not guarantee better forensic performance; (3) Any use of automatic restoration in a forensic pipeline should be fully documented, including the specific models used, their configuration, and when they are applied. Downstream practitioners, courts, and auditors need to know whether an image has been algorithmically altered and why; and (4) Our failure-prediction scores could be exposed to human examiners as an additional piece of meta-evidence—e.g., flagging lineups as high-risk for recognition failure and suggesting when additional human scrutiny or supplementary evidence is warranted.

In the broader policy debate around facial recognition, our results add nuance to the question of whether current systems are good enough for forensic use. They show that, even with sophisticated enhancement tools and careful engineering, accuracy gaps in realistic conditions persist, and that naive attempts to fix difficult images can backfire. This strengthens arguments for conservative deployment, strict use policies, and rigorous, context-specific validation.

Several limitations of our study should be acknowledged: (1) Our evaluation relies on a curated subset of CASIA-WebFace, which, while large and diverse, is not a perfect proxy for all forensic imagery (e.g., bodycam footage with lens distortion and motion blur, or low-light CCTV with extreme compression); (2) We concentrate on two widely used recognition models, ArcFace and FaceNet. Other architectures—especially more recent or proprietary systems—may respond differently to the same restoration pipeline or exhibit different sensitivities to artifacts and (3) Although our dataset includes demographic variation, we do not explicitly analyze performance differences across demographic groups. It remains an open question whether restoration and failure-prediction methods disproportionately help or harm certain populations.

These limitations suggest caution in directly extrapolating our quantitative results to all real-world deployments. Instead, we view our framework and findings as a template for how such systems should be evaluated and stress-tested.

In sum, our findings challenge the intuition that more restoration is always better. We show that modern head-pose correction and image restoration methods, when naively applied, can severely undermine the reliability of facial recognition systems in exactly the kinds of difficult, real-world conditions where they are most needed. At the same time, we demonstrate that a carefully calibrated, selectively applied pipeline, guided by a high-precision failure-prediction model, can achieve meaningful improvements with limited downside. Forensic facial recognition, therefore, does not simply need better images; it needs better, context-aware decisions about when and how to intervene on those images. Our framework offers one concrete step in that direction.

## References

- [1] Joy Buolamwini and Timnit Gebru. Gender shades: Intersectional accuracy disparities in commercial gender classification. In *Conference on Fairness, Accountability and Transparency*, pages 77–91. PMLR, 2018. [1](#)
- [2] Zhiyi Cheng, Xiatian Zhu, and Shaogang Gong. Low-resolution face recognition. In *14th Asian Conference on Computer Vision*, pages 605–621. Springer, 2019. [1](#)
- [3] Jiankang Deng, Jia Guo, Niannan Xue, and Stefanos Zafeiriou. Arcface: Additive angular margin loss for deep face recognition. In *International Conference on Computer Vision and Pattern Recognition*, pages 4690–4699, 2019. [1](#)
- [4] Abdallah Dib, Gaurav Bharaj, Junghyun Ahn, Cédric Thébault, Philippe Gosselin, Marco Romeo, and Louis Chevallier. Practical face reconstruction via differentiable ray tracing. In *Computer Graphics Forum*, volume 40, pages 153–164. Wiley Online Library, 2021. [1](#)
- [5] Abdallah Dib, Cédric Thébault, Junghyun Ahn, Philippe-Henri Gosselin, Christian Theobalt, and Louis Chevallier. Towards high fidelity monocular face reconstruction with rich reflectance using self-supervised learning and ray tracing. In *Proceedings of the IEEE/CVF International Conference on Computer Vision (ICCV)*, pages 12819–12829, October 2021. [1](#), [4](#)
- [6] Matthijs Douze, Alexandr Guzhva, Chengqi Deng, Jeff Johnson, Gergely Szilvasy, Pierre-Emmanuel Mazaré, Maria Lomeli, Lucas Hosseini, and Hervé Jégou. The faiss library. *arXiv preprint arXiv:2401.08281*, 2024. [3](#)
- [7] Yeong-Joon Ju, Gun-Hee Lee, Jung-Ho Hong, and Seong-Whan Lee. Complete face recovery gan: Un-supervised joint face rotation and de-occlusion from a single-view image. In *Proceedings of the IEEE/CVF Winter Conference on Applications of Computer Vision (WACV)*, pages 3711–3721, January 2022. [1](#), [5](#)
- [8] Davis E King. Dlib-ml: A machine learning toolkit. *The Journal of Machine Learning Research*, 10:1755–1758, 2009. [6](#)
- [9] Adam Kortylewski, Bernhard Egger, Andreas Schneider, Thomas Gerig, Andreas Morel-Forster, and Thomas Vetter. Analyzing and reducing the damage of dataset bias to face recognition with synthetic data. In *International Conference on Computer Vision and Pattern Recognition Workshop*, 2019. [1](#)
- [10] Dilip Krishnan, Terence Tay, and Rob Fergus. Blind deconvolution using a normalized sparsity measure. In *CVPR 2011*, pages 233–240. IEEE, 2011. [4](#)
- [11] Camillo Lugaresi, Jiuqiang Tang, Hadon Nash, Chris McClanahan, Esha Uboweja, Michael Hays, Fan Zhang, Chuo-Ling Chang, Ming Yong, Juhyun Lee, Wan-Teh Chang, Wei Hua, Manfred Georg, and Matthias Grundmann. MediaPipe: A framework for perceiving and processing reality. In *Third Workshop on Computer Vision for AR/VR at IEEE Computer Vision and Pattern Recognition*, 2019. [6](#)

- [12] Vincent Manancourt. Controversial US facial recognition technology likely illegal, EU body says. *Politico*, 2022. [1](#)
- [13] Justin Norman, Shruti Agarwal, and Hany Farid. An evaluation of forensic facial recognition, 2023. [1](#), [2](#)
- [14] Justin Norman and Hany Farid. An investigation into the impact of ai-powered image enhancement on forensic facial recognition. In *Proceedings of the IEEE/CVF Conference on Computer Vision and Pattern Recognition (CVPR) Workshops*, pages 4306–4314, June 2024. [1](#), [2](#), [4](#), [9](#)
- [15] Alice J O’Toole and Carlos D Castillo. Face recognition by humans and machines: Three fundamental advances from deep learning. *Annual Review of Vision Science*, 7:543–570, 2021. [1](#)
- [16] Fabian Pedregosa, Gaël Varoquaux, Alexandre Gramfort, Vincent Michel, Bertrand Thirion, Olivier Grisel, Mathieu Blondel, Peter Prettenhofer, Ron Weiss, Vincent Dubourg, Jake Vanderplas, Alexandre Passos, David Cournapeau, Matthieu Brucher, Matthieu Perrot, and Édouard Duchesnay. Scikit-learn: Machine Learning in Python. *Journal of Machine Learning Research*, 12:2825–2830, 2011. [7](#)
- [17] P Jonathon Phillips, Amy N Yates, Ying Hu, Carina A Hahn, Eilidh Noyes, Kelsey Jackson, Jacqueline G Cavazos, Géraldine Jeckeln, Rajeev Ranjan, Swami Sankaranarayanan, et al. Face recognition accuracy of forensic examiners, superrecognizers, and face recognition algorithms. *Proceedings of the National Academy of Sciences*, 115(24):6171–6176, 2018. [1](#)
- [18] Inioluwa Deborah Raji, Timnit Gebru, Margaret Mitchell, Joy Buolamwini, Joonseok Lee, and Emily Denton. Saving face: Investigating the ethical concerns of facial recognition auditing. In *AAAI/ACM Conference on AI, Ethics, and Society*, pages 145–151, 2020. [1](#)
- [19] Marcus Smith and Seumas Miller. The ethical application of biometric facial recognition technology. *AI & Society*, 37(1):167–175, 2022. [1](#)
- [20] Alice Towler, James D Dunn, Sergio Castro Martínez, Reuben Moreton, Fredrick Eklöf, Arnout Ruifrok, Richard I Kemp, and David White. Diverse types of expertise in facial recognition. *Scientific Reports*, 13(1):11396, 2023. [1](#)
- [21] Mei Wang and Weihong Deng. Deep face recognition: A survey. *Neurocomputing*, 429:215–244, 2021. [1](#)
- [22] Cedric Deslandes Whitney and Justin Norman. Real risks of fake data: Synthetic data, diversity-washing and consent circumvention. In *The 2024 ACM Conference on Fairness, Accountability, and Transparency*, pages 1733–1744, 2024. [2](#)
- [23] Dong Yi, Zhen Lei, Shengcai Liao, and Stan Z Li. Learning face representation from scratch. arXiv:1411.7923, 2014. [2](#)
- [24] Xi Yin, Xiang Yu, Kihyuk Sohn, Xiaoming Liu, and Manmohan Chandraker. Towards large-pose face frontalization in the wild. In *Proceedings of the IEEE International Conference on Computer Vision*, pages 3990–3999, 2017. [1](#)
- [25] Syed Waqas Zamir, Aditya Arora, Salman Khan, Munawar Hayat, Fahad Shahbaz Khan, and Ming-Hsuan Yang. Restormer: Efficient transformer for high-resolution image restoration. In *International Conference on Computer Vision and Pattern Recognition*, pages 5728–5739, 2022. [4](#)
- [26] Shangchen Zhou, Kelvin Chan, Chongyi Li, and Chen Change Loy. Towards robust blind face restoration with codebook lookup transformer. In *Advances in Neural Information Processing Systems*, volume 35, pages 30599–30611, 2022. [1](#), [5](#)